Haloperidol-Based Irreversible Inhibitors of the HIV-1 and HIV-2 Proteases

James J. De Voss, Zhihua Sui, Dianne L. DeCamp, Rafael Salto, Lilia M. Babé, Charles S. Craik, and Paul R. Ortiz de Montellano*

Department of Pharmaceutical Chemistry, School of Pharmacy, University of California, San Francisco, California 94143-0446

Received November 15, 1993•

The proteases expressed by the HIV-1 and HIV-2 viruses process the polyproteins encoded by the viral genomes into the mature proteins required for virion replication and assembly. Eight analogs of haloperidol have been synthesized that cause time-dependent inactivation of the HIV-1 protease and, in six cases, HIV-2 protease. The IC_{50} values for the analogues are comparable to that of haloperidol itself. Enzyme inactivation is due to the presence of an epoxide in two of the analogues and carbonyl-conjugated double or triple bonds in the others. Irreversible inactivation is confirmed by the failure to recover activity when one of the inhibitors is removed from the medium. At pH 8.0, the agents inactivate the HIV-1 protease 4–80 times more rapidly than the HIV-2 protease. Faster inactivation of the HIV-1 protease is consistent with alkylation of cysteine residues because the HIV-1 protease has four such residues whereas the HIV-2 protease has none. Inactivation of the HIV-2 protease requires modification of non-cysteine residues. The similarities in the rates of inactivation of the HIV-2 protease by six agents that have intrinsically different reactivities toward nucleophiles suggest that the rate-limiting step in the inactivation process is not the alkylation reaction itself. At least five of the agents inhibit polyprotein processing in an *ex vivo* cell assay system, but they are also toxic to the cells.

The HIV-1 aspartyl protease (HIV-1 PR), for which a high-resolution three-dimensional structure is available, is a dimer of two identical subunits of 99 amino acids each.[1-4] The HIV-2 protease (HIV-2 PR) is 39–44% identical in sequence and, as shown by X-ray crystallography, is an analogous dimer.[5] The proteases are required to process the polypeptides encoded by the viral *gag* and *pol* genes and are therefore essential for viral maturation.[6] Mutation of the catalytic aspartate at position 25 of HIV-1 PR yields an inactive enzyme and results in noninfectious virions.[1,7] The protease is therefore under intense investigation as a target for the development of therapeutic agents for AIDS. Peptides that inhibit the protease *in vitro* with nanomolar K_I values have been synthesized and shown to inhibit *gag* polyprotein processing[8-10] and to reduce viral infectivity in cultured T4 cells.[11] However, the pharmacokinetic difficulties inherent in the use of peptide-based agents as pharmaceutical agents[12] make the development of non-peptide inhibitors of the HIV proteases highly desirable. A structure-based, computer-assisted search procedure has identified haloperidol (1), a clinically employed antipsychotic agent that readily crosses the blood–brain barrier,[13] as an inhibitor of HIV-1 PR with apparent K_I = 100 μM (IC_{50} = 125 μM).[14] The crystal structure of a thioketal derivative of haloperidol bound in the active site of HIV-1 PR has been determined to high resolution.[15] The K_I value of haloperidol, however, is approximately 1000 times higher than the serum concentrations achieved in patients treated with the drug.[13,16] Haloperidol is toxic at elevated concentrations and therefore is not itself a viable drug for the treatment of AIDS. Nevertheless, its specificity for the HIV proteases,[14] its attractive pharmacokinetic properties, and its synthetic flexibility make it an attractive lead structure.

The catalytic mechanisms of aspartyl proteases involve the concerted action of two aspartyl carboxyl groups, only one of which is protonated.[17,18] Although details of the catalytic mechanisms of the HIV proteases remain to be settled, kinetic and isotope studies indicate that the HIV-1 PR catalytic mechanism is similar to that of the other aspartyl proteases.[19,20] In this mechanism, the protonated aspartyl hydrogen bonds to the amide carbonyl of the substrate and the unprotonated aspartyl to a water molecule. Transfer of the hydrogen from the aspartyl to the carbonyl group coupled with addition of the water molecule gives a *gem*-diol intermediate. One of the two hydrogens of the water is retained and is shared by the aspartyl groups. The *gem*-diol intermediate is then cleaved, again with the help of the two differentially protonated aspartyl groups. The push–pull aspects of this mechanism, in which one aspartate functions as a proton donor and the other as a base, suggest that the HIV proteases should be sensitive to inactivation by functionalities that are activated by protonation toward nucleophilic additions. Indeed, aspartyl proteases, including HIV-1 PR,[21] are inactivated by 1,2-epoxy-3-(*p*-nitrophenoxy)propane. In the case of pepsin, inactivation is due to alkylation of an aspartate residue,[22,23] and a similar mechanism has been proposed for HIV-1 PR on the basis of the pH profile of the inactivation.[21] Furthermore, cerulenin, an epoxide-containing inhibitor of fatty acid biosynthesis, has been found to irreversibly inhibit the HIV-1 protease.[24,25] Although the IC_{50} value (2.5 mM) for cerulenin is disappointingly high and no information is available on the inhibitory mechanism,[24,25] irreversible inhibition is consistent with aspartate-catalyzed protein alkylation. Inactivation could also result from alkylation of one or more sulfhydryl groups, however, because HIV-1 PR is known to be inactivated by sulfhydryl reagents.[21] These results suggest that incorporation of an epoxide into a haloperidol analogue may yield an irreversible inhibitor with high affinity for HIV-1 PR and/or HIV-2 PR.[26] However, the chemical reactivity of epoxides and the existence of enzymes that specifically hydrolyze

• Abstract published in *Advance ACS Abstracts*, February 1, 1994.

0022-2623/94/1837-0665$04.50/0

Scheme 1

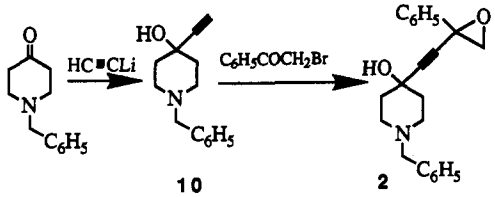

Scheme 2

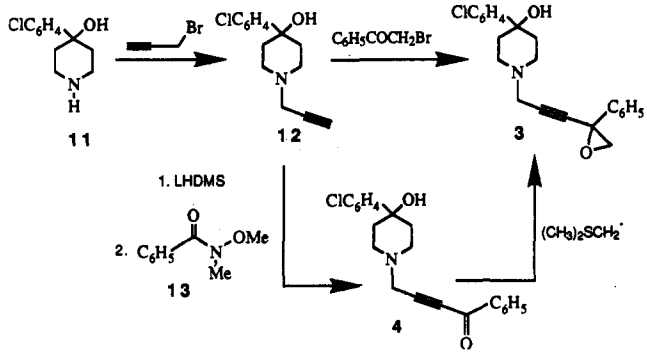

epoxides to diols[27] diminish the potential *in vivo* efficacy of epoxides as HIV protease inhibitors. We have therefore synthesized and examined not only epoxide analogues **2** and **3**, but also haloperidol derivatives with an ynone (**4–6**) or α,β-unsaturated ketone (**7–9**) as the alkylating functionality.

Results and Discussion

Synthesis of Epoxide 2. The acetylenic alcohol **10** was obtained in approximately 66% yield by addition of lithium acetylide to commercially available *N*-benzyl-4-piperidinone (Scheme 1). Subsequent condensation of **10** with bromoacetophenone provided epoxide **2** in 62% yield.

Synthesis of Epoxide 3 and Ynone 4. Epoxide **2** is not truly a haloperidol analogue because the piperidine ring is reversed so that the acyclic chain is bound to the hydroxyl-substituted carbon and the piperidine nitrogen is distal to the acyclic chain. An approach similar to that used to prepare **2** was initially employed to produce epoxide **3**, a much closer haloperidol analogue. Reaction of piperidine **11** with propargyl bromide in DMF provided *N*-(2-propynyl)piperidine **12** in 98% yield (Scheme 2). However, there was little or no reaction of the dianion of **12**, generated in tetrahydrofuran with lithium hexamethyldisilazide, with bromoacetophenone. The failure of this reaction is presumably due to enolization of the bromoacetophenone under the basic reaction conditions. The reaction also did not take place when the magnesium salt of **12** was generated by reaction with ethylmagnesium bromide. Cerium salts of carbon-based anions in general,[28] and acetylides in particular, are known to facilitate addition reactions to easily enolized ketones. The cerium salt of **12** was therefore prepared by metal exchange of the dilithium salt. Reaction of the cerium salt with bromoacetophenone resulted in the formation of a poorly separable, equimolar mixture of **3** and unreacted starting material.

An alternative, more practical synthesis of **3** that emerged after a number of other approaches were examined involves conversion of **12** to the dilithium salt with lithium hexamethyldisilazide followed by reaction with amide **13**[29] to give ynone **4** in good yield. Reaction of **4** with dimethylsulfonium methylide[30] provides epoxide **3** in approximately 38% purified yield.

Scheme 3

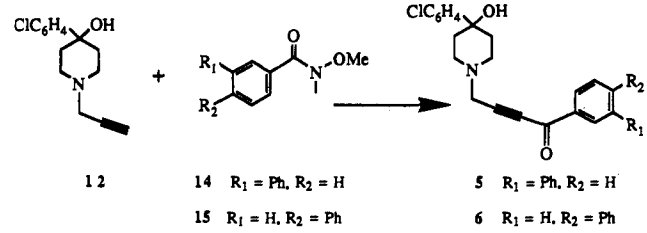

Scheme 4

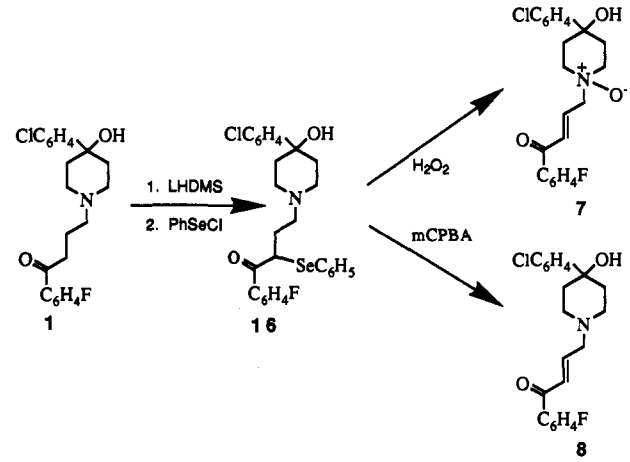

The synthetic route in Scheme 2 has the advantage that it provides not only epoxide **3** but also acetylenic ketone **4**. Ynone **4** is a desirable target molecule for two reasons: (a) it could potentially have a higher affinity for the enzyme than haloperidol due to the smaller loss of entropy associated with binding of the rigid chain of **4** compared to the flexible butyrophenone chain of haloperidol and (b) the acetylenic ketone function is a good Michael acceptor and is more resistant to metabolic deactivation than the epoxide function.

Synthesis of Ynones 5 and 6. Extensive structure–activity studies of haloperidol and its analogues have shown that replacement of the fluorophenyl ring of haloperidol with a biphenyl moiety substantially improves HIV protease inhibitory activity (unpublished work). The ynones with a *m*- (**5**) or *p*-biphenyl group (**6**) replacing the phenyl group of **4** were therefore synthesized to determine whether the increased affinity associated with the biphenyl group in the haloperidol series would also be effective in the ynone derivatives. Compounds **5** and **6** were synthesized by condensation of **2** with **14** or **15**, respectively (Scheme 3).

Synthesis of α,β-Unsaturated Ketones 7 and 8. A double bond was introduced adjacent to the carbonyl group of haloperidol as shown in Scheme 4. Formation of the enolate of haloperidol (**1**) by reaction with lithium hexamethyldisilazide followed by reaction with phenylselenyl chloride yielded the α-phenylselenyl-substituted compound **16** in 73% yield (Scheme 4). Oxidative elimination of the phenylselenyl group with H_2O_2 gave **7** in 66% yield. In addition to the oxidative elimination, the reaction with H_2O_2 converts the piperidine nitrogen to the *N*-oxide, but this is not an undesirable transformation because the electron-withdrawing effect of the *N*-oxide is likely to increase the reactivity of the α,β-unsaturated double bond. Analogue **8** with an intact piperidine nitrogen was obtained by oxidizing **16** with 1 equiv of *m*-chloroperbenzoic acid rather than H_2O_2.

Synthesis of α,β-Unsaturated Ketone 9. The reac-

Scheme 5

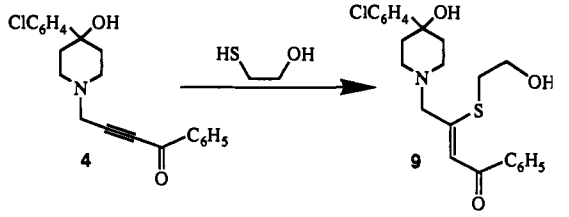

Table 1. Rates of Reaction of Selected Inhibitors with Nucleophiles as a Function of pH

structure	nucleophile	pH (37 °C)	k_2 (M^{-1} min^{-1})[a]
4 (rapid phase)	GSH[b]	7.8	5.2 ± 0.3
	GSH	8.8	16.4 ± 0.9
	GSH	9.7	12.6 ± 1.3
	GSH	10.6	13.8 ± 0.9
4 (slow phase)	GSH	7.8	0.5 ± 0.01
4	NaOAc	7.8	1.5 ± 0.1
7	GSH	7.8	6.6 ± 0.2
	GSH	8.8	26.7 ± 1.2
	GSH	9.7	97.5 ± 3.5
	GSH	10.6	92.8 ± 2.6
9	GSH	7.8	0.6 ± 0.07

[a] No changes are observed in the electronic absorption spectra of 4, 7, or 9 when incubated in the absence of GSH or NaOAc, indicating that water addition to this compounds does not occur at a significant rate under the present conditions. [b] GSH = glutathione.

tion of β-mercaptoethanol with ynone 4 was examined as a possible model for the reaction involved in enzyme inactivation (Scheme 5). The product isolated from the reaction, which retains a reactive α,β-unsaturated ketone functionality, was itself examined as an inactivating agent. The NMR spectrum of the product indicates that only one of the two possible isomers of 9 is formed. On the basis of the observation that irradiation of the vinyl proton results in NOE enhancement of the methylene protons adjacent to the piperidine nitrogen, the product is assigned the indicated structure.

Addition of Nucleophiles to α,β-Unsaturated Carbonyl Compounds. The rates of addition of glutathione to ynone 4 and enones 7 and 9 have been measured spectrophotometrically to establish a baseline against which to compare the reactions of the same agents with protein nucleophiles. Glutathione was used for these studies because it is a water-soluble peptide that should mimic reasonably well the reactivity of surface cysteine residues (*vide infra*). The rate of addition of glutathione to 4 triples as the pH is raised from 7.8 to 8.8 but decreases slightly when the pH is raised further from 8.8 to 9.7 or 10.6 (Table 1). In contrast, addition of glutathione to enone 7 quadruples when the pH is raised from 7.8 to 8.8 and rises a further 3.5-fold when the pH is raised from 8.8 to 9.7 (Table 1). The rate remains essentially unchanged, however, when the pH rises from 9.7 to 10.6. The sharp increase in the reaction rate between pH 7.8 and 9.7 observed with enone 7 clearly suggests that the nucleophile involved in the reaction is the thiolate anion of glutathione (pK_a = 8.7). The pH profile of the reaction in the case of ynone 4 is consistent with this inference but is complicated by the fact that the rate decreases slightly in going from pH 8.8 to 9.7. This decrease may reflect a decrease in the reactivity of the ynone function caused by deprotonation of the piperidine nitrogen in 4, a complication not observed with 7 because the piperidine nitrogen is present as the *N*-oxide. The pK_a value of the piperidine nitrogen in 4 is not known but would be expected to be slightly lower than that of haloperidol (pK_a = 8.3)[31] due to the electron-withdrawing effect of the triple bond.

Scheme 6

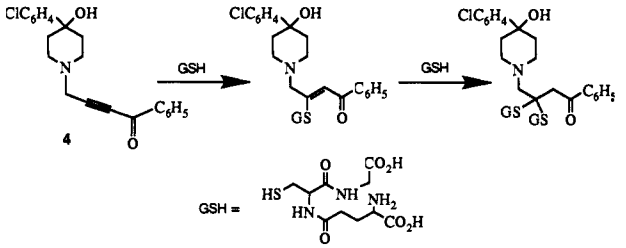

Table 2. Inhibition of the HIV-1 and HIV-2 Proteases

	IC_{50} (μM)		k_{inact} (min^{-1} × 10^3)	
structure	HIV-1	HIV-2	HIV-1	HIV-2
1	125[a]	140[a]	NI[b]	NI
2	725	350	63 ± 1[c]	NI
3	150	235	184 ± 2[c]	5.70 ± 0.14[c]
4	20	33	186 ± 17	3.78 ± 0.09
5	63	44	317 ± 22	3.89 ± 0.18
6	100	35	309 ± 3	NI
7	30	40	86 ± 5	4.33 ± 0.25
8	80	100	374 ± 4	6.15 ± 0.28
9	140	133	11 ± 1	3.16 ± 0.23

[a] The values for haloperidol (1) are from ref 13. [b] NI = no detectable irreversible inhibition. [c] Rate calculations for the epoxides are not corrected for changes in concentration due to chemical hydrolysis during the incubation. The experimental rate constants are therefore approximate and are underestimates of the actual values.

Addition of glutathione to 4 is actually biphasic. The rate of the slow reaction is one-tenth of the rate of the initial fast reaction (Table 1). The slow rate of addition is attributed to addition of a second molecule of glutathione to the β-mercapto enone produced by the first addition (Scheme 6). Strong support for this interpretation of the biphasic kinetics is provided by the fact that the rate of addition of glutathione to β-mercapto enone 9 is essentially identical to that of the slow phase of the reaction with 4 (Table 1). Addition of glutathione to 9 or to the product formed from 4 by addition of one glutathione (Scheme 6) is, as expected, considerably slower than addition to enone 7 due to the presence of two β-substituents on the double bond.

Addition of acetate to 4 is slower, as expected, than addition of glutathione (Table 1). The acetate anion is a much poorer nucleophile than a thiolate anion. Alkylation of cysteine sulfhydryl groups in a protein is therefore favored by a factor of up to 10 over alkylation of aspartate carboxylates unless specific binding of the inhibitor raises its effective concentration in the vicinity of the aspartates, the reactivity of the aspartates is enhanced by protein interactions, or the cysteines are masked.

***In Vitro* Inhibition of the HIV Proteases.** Analogues 2–9 are inhibitors of HIV-1 PR with IC_{50} = 725, 150, 20, 63, 100, 30, 80, and 140 μM, respectively (Table 2). The analogues also inhibit HIV-2 PR with IC_{50} = 350, 235, 33, 44, 35, 40, 100, and 133 μM, respectively (Table 2). These values are to be compared with IC_{50} = 125 and 140 μM, respectively, for inhibition of HIV-1 PR and HIV-2 PR by haloperidol (1).[14] More importantly, all eight compounds cause time-dependent irreversible inactivation of HIV-1 PR. A striking difference is observed in the rates of inactivation of HIV-1 PR and HIV-2 PR by the inhibitory agents (Table 2). With the exception of compound 9, HIV-1 PR is inactivated 10–100 times faster than HIV-2 PR. Compound 9 also inactivates HIV-1 PR more rapidly than HIV-2 PR, but the rates only differ by approximately a factor of 4. Although all the compounds inactivate HIV-1

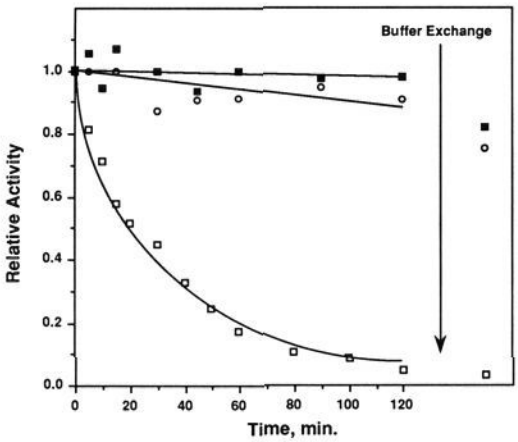

Figure 1. Irreversible inactivation of HIV-1 PR by **3**. HIV-1 PR (100 μg, 400 μL final volume) was preincubated in the presence of 100 μM **3** (□), 100 μM haloperidol (■) or no inhibitor (○) at 25 °C in 50 mM Hepes buffer (pH 8.0) containing 1 M NaCl, 1 mM EDTA, and 5% DMSO. At various times, aliquots were removed and assayed for activity as described in the Experimental Section. After 2 h preincubation the samples were exchanged against the same buffer without inhibitor using centricon 10 microconcentrators and assayed. After buffer exchange, the calculated concentration of **3** and haloperidol was less than 0.2 μM.

PR, compounds **2** and **6** do not detectably inactivate HIV-2 PR.

In order to assess the irreversibility of the inactivation reaction, HIV-1 PR was incubated alone, with haloperidol (**1**), or with compound **3** (Figure 1). Aliquots of the three preincubation mixtures were removed at time points up to 100 min, and their catalytic activity was assayed. After a 120-min preincubation, the three preincubation mixtures were exchanged against buffer containing neither haloperidol nor compound **3** using centricon 10 microconcentrators (Amicon). The activity of each of the solutions was then determined. The concentration of haloperidol or **3** after the exchange step was calculated to be less than 0.2 μM. The results clearly show that HIV-1 PR loses no more than 10% of its catalytic activity when incubated alone or with haloperidol under these conditions (Figure 1). In contrast, the enzyme incubated with **3** exhibits clear time-dependent loss of activity far in excess of this background level. Furthermore, comparison of the 120-min activities measured before and after buffer exchange clearly shows that the activity of HIV-1 PR inactivated by **3** is not recovered when the inhibitor is removed from the medium (Figure 1). The inhibition caused by **3** is therefore irreversible. In a similar manner, compounds **4–9** cause time-dependent loss of the catalytic activity of HIV-1 PR and, except for **6**, also of HIV-2 PR.

***Ex Vivo* Inhibition of Viral Polyprotein Processing.** The ability of the agents to inhibit viral polyprotein processing has been investigated (Table 3). The compound which showed the most significant inhibition at the lowest tolerable concentration was **2**. This compound was used in further experiments to correlate the decrease in capsid protein processing with infectivity of progeny virus. The virus particles obtained after treatment of HIV-producing COS7 cells were used to infect HeLa cells expressing CD4. The number of infectious particles was calculated by counting the colonies of infected HeLa-T4 cells. Figure 2 shows the effect of increasing concentrations of **2** on the virus titer. The concentration of p24 capsid protein in these samples and the cell viability at each concentration

Table 3. *Ex Vivo* Activity of the Irreversible HIV-1 Protease Inhibitors

structure	LD_{50} (4 h) (μM)	LD_{50} (24 h) (μM)	reduction of p24 IC_{50} (μM)
2	70	40	25
3	120	50	50
4	15	<10	nt
5	35	nt	35
6	10	<5	nt
7	250	200	75
8	20	<10	15
9	>250	75	nt
U75875[b]	>100	45	0.75

[a] nt = not tested. [b] Peptidomimetic inhibitor U75875 included as a control.[38]

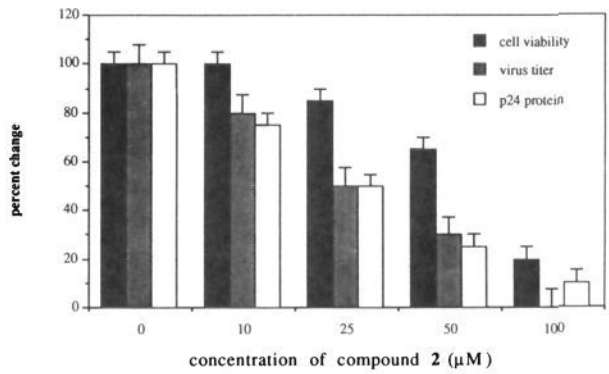

Figure 2. Inhibition of HIV-1 polyprotein processing, virus replication, and cell viability by increasing doses of compound **2**.

are also shown. A decrease of 50% in both p24 protein and viral infectivity is observed at a 25 μM concentration of **2**, a concentration at which the viability of cells is only decreased by 15%. At higher concentrations of **2**, the efficacy of the drug increases but so do the cytotoxic effects. Analysis of the proteins in similar viral preparations reveals a similar pattern of p24 reduction and a concomitant increase in the precursor proteins (data not shown). These results confirm the specific inhibitory effect of this new class of haloperidol derivatives on HIV-1 PR in intact cells.

Conclusions

Haloperidol analogues incorporating a reactive functionality into the four-carbon chain readily inactivate both HIV-1 PR and HIV-2 PR. Irreversible inhibition of HIV-1 PR is explicitly demonstrated for compound **3** by the demonstration that the loss of activity is not reversed when the inhibitor is removed from the medium (Figure 1). For each agent, inactivation of HIV-1 PR is considerably faster than inactivation of HIV-2 PR, although the differences range from a factor of 4 (for **9**) to a factor of 75 (for **5**). Faster inactivation of HIV-1 PR is readily explained if that enzyme is primarily inactivated by alkylation of one of the four sulfhydryl groups in the homodimer because there are no sulfhydryls in HIV-2 PR. The crystal structure shows that two of the symmetrically disposed sulfhydryl groups (Cys 95 and 195) are at the subunit interface and are solvent inaccessible. The other two (Cys 67 and 167) are fully exposed on the exterior of the protein (Figure 3). None of the sulfhydryl groups is in the active site. Inactivation of HIV-1 PR, if primarily mediated by alkylation of the sulfhydryl groups, as appears likely, requires that the enzyme be disabled by a non-active-site modification. This would require, for example, that

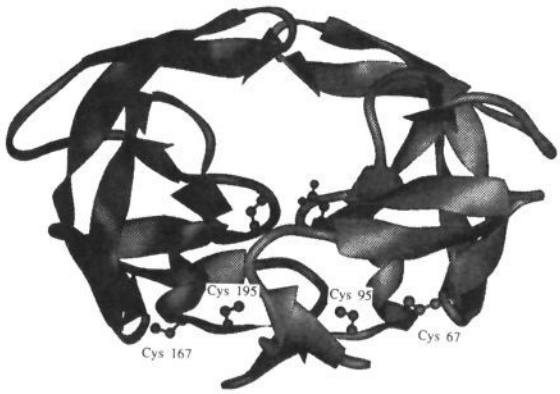

Figure 3. Backbone structure of the HIV-1 protease indicating the location of the four sulfhydryl groups. The catalytic aspartic acid residues are, as shown, at the bottom of the active-site cavity.

sulfhydryl alkylation interfere with subunit association or the motion required to close the flaps over the active site when substrate is bound. A sulfhydryl alkylation mechanism is consistent with the fact that HIV-1 PR is inactivated by the sulfhydryl-selective reagents *N*-ethylmaleimide and iodoacetamide.[21] Detailed studies of the site of alkylation confirm that irreversible inhibition of HIV1-PR involves alkylation of sulfhydryl groups as well as active-site residues.[32]

Inactivation of HIV-2 PR, which has no sulfhydryl groups, is likely to involve modification of the active-site aspartates or alternative active-site residues. This inactivation reaction may also occur with HIV-1 PR but is dominated in that enzyme by a more rapid inactivation mechanism involving sulfhydryl group alkylation. Except for the fact that two of the agents do not detectably inactivate the enzyme, the differences in the rates of inactivation of HIV-2 PR by the various agents are relatively small (Table 1). It is surprising, for example, that ynone **4** and β-mercapto enone **9** inactivate the enzyme at approximately the same rate, given the clear difference in the rates of addition of nucleophiles to the two compounds (Table 1). The similarities in the rates of inactivation suggest that the rate-limiting step in the inactivation reaction is something other than addition of an enzyme nucleophile to the reactive epoxide or unsaturated ketone functionalities in the inhibitors. It is possible, for example, that the protease undergoes a rate-limiting conformational change that exposes the nucleophile that is alkylated, but detailed studies of the inactivation mechanism are required to further characterize the inactivation process.

At least five of the inhibitors exhibit detectable activity as inhibitors of polyprotein processing in cell culture, but all of the compounds are too toxic to the cells to be of therapeutic value. The development of practical, haloperidol-based, irreversible inhibitors of the HIV proteases depends on further successful modification of the haloperidol framework to improve the specificity and decrease the toxicity of the inhibitors.

Experimental Section

General. Melting points were determined with a Thomas capillary melting point apparatus and are uncorrected. Proton and carbon NMR spectra were obtained at 300 and 75 MHz, respectively, on a GE QE-300 instrument. Infrared spectra were recorded on a Nicolet 5DX FT-IR. Mass spectra were measured wtih a VG-70 mass spectrometer. Elemental analyses were performed by the Microanalysis laboratory, University of California, Berkeley. Tetrahydrofuran and ether were dried over sodium/benzophenone and distilled under argon immediately prior to use.

***N*-Benzyl-4-ethynyl-4-piperidinol (10).** Lithium acetylide ethylenediamine complex (1.0 g, 1.8 equiv) was suspended in dry tetrahydrofuran and the mixture cooled to 0 °C under argon before *N*-benzyl-4-piperidinone (1.0 g, 5.28 mmol) in dry tetrahydrofuran (5 mL) was added dropwise to the stirred mixture. After the mixture was stirred overnight, the reaction was quenched with saturated ammonium chloride solution (30 mL) and the aqueous phase was extracted with ethyl acetate (3 × 100 mL). The combined organic extracts were dried ($MgSO_4$), and the solvent was removed under reduced pressure. The crude material was purified by flash column chromatography (SiO_2, 45–55% ethyl acetate/hexane) to give the starting piperidone (343 mg) and **10** as an oil (747 mg, 65.7% or 100% based on recovered starting material): IR ($CHCl_3$) 3409, 3304, 3016, 2952, 2812, 2770, 1497 cm^{-1}; ^1H NMR (300 MHz, $CDCl_3$) δ 1.80–1.98 (m, 4H, 2 CH_2CH_2N), 2.37–2.44 (m, 2 H, 2 ax CH_2CH_2N), 2.49 (s, 1H, acetylenic CH), 2.56 (br s, 1 H, OH), 2.60–2.70 (m, 2 H, 2 eq CH_2CH_2N), 3.52 (s, 2 H, $CH_2C_6H_5$), and 7.23–7.35 ppm (m, 5 H, C_6H_5); ^{13}C NMR (75 MHz, $CDCl_3$) δ 38.88, 49.89, 62.64, 66.41, 72.57, 87.06, 126.95, 127.12, 128.04, and 138.22 ppm; MS *m/z* (CI) 216 (MH^+, 100), 214 (15), 126 (22), 108 (13) and 91 (C_7H_7, 18); HRMS calcd for $C_{14}H_{17}NO$ 215.1310, found 215.1287.

***N*-Benzyl-4-(3′,4′-epoxy-3′-phenylbut-1′-ynyl)-4-piperidinol (2).** *N*-Benzyl-4-ethynyl-4-piperidinol (109 mg, 0.506 mmol) was dissolved in dry tetrahydrofuran (5 mL) and lithium hexamethyldisilazide (1.012 mL of a 1 M tetrahydrofuran solution, 2 equiv) was added dropwise under argon at 0 °C to the stirred solution. After 1 h, phenacyl bromide (101 mg, 0.506 mmol) was added and the reaction was allowed to warm to room temperature and stirred overnight. It was then quenched with saturated ammonium chloride (20 mL), and the aqueous phase was extracted with ethyl acetate (2 × 20 mL). The combined organic extracts were dried, and the solvent was removed under vacuum. The oil thus obtained was purified by flash column chromatography (SiO_2, 60% ethyl acetate/hexane) to give **2** (105 mg, 62%) contaminated with a small amount of the starting material. This material was further purified by flash column chromatography (SiO_2, 5% 2-propanol/dichloromethane) to give pure **2**: IR ($CHCl_3$) 3009, 2952, 2812, 2770, 1954, 1602, and 1497 cm^{-1}; ^1H NMR (300 MHz, $CDCl_3$) δ 1.81–1.98 (m, 4H, 2 CH_2CH_2N), 2.37–2.43 (m, 2 H, 2 ax CH_2CH_2N), 2.60–2.75 (m, 2 H, 2 eq CH_2CH_2N), 3.01, 3.38 (AB q, 2 H, J_{AB} = 6 Hz, CH_2O), 3.52 (m, 2 H, $C_6H_5CH_2$), and 7.23–7.48 ppm (m, 10 H, 2 C_6H_5); ^{13}C NMR (75 MHz, $CDCl_3$) δ 39.00, 49.98, 50.86, 59.18, 62.69, 66.72, 82.30, 87.52, 125.44, 127.03, 128.19, 128.37, 128.41, 129.08, 136.91, and 138.20 ppm; MS *m/z* (CI) 331 (MH^+, 50), 275 (32), 190 (35), 115 (32), and 91 (C_7H_7, 100); HRMS calcd for $C_{22}H_{23}NO_2$ 333.1729, found 333.1732.

***N*-Propargyl-4-(4′-chlorophenyl)-4-piperidinol (12).** Potassium carbonate (1.10 g, 8 mmol) and propargyl chloride (360 μL, 1.05 equiv) were added to a solution of 4-(4′-chlorophenyl)-4-piperidinol (**11**) (1.0 g, 4.7 mmol) in DMF (10 mL), and the solution was stirred overnight at room temperature. The reaction mixture was then diluted with ether (60 mL), washed sequentially with half-saturated brine (2 × 20 mL) and brine (20 mL), dried, and evaporated under reduced pressure to yield **12** as a pale yellow solid (1.16 g, 98%) that could be recrystallized from CH_2Cl_2/hexane for analysis: mp 127.5–128 °C; IR ($CHCl_3$) 3304, 2945, 2826, 1497, and 1096 cm^{-1}; ^1H NMR (300 MHz, $CDCl_3$) δ 1.76 (ddd, 2 H, J = 12, 5, 2.8 Hz, 2 eq CH_2CH_2N), 2.15 (td, 2 H, J = 12.5, 4 Hz, 2 ax CH_2CH_2N), 2.28 (t, 1H, J = 2 Hz, acetylenic CH), 2.67 (td, 2 H, J = 12, 2.5 Hz, 2 ax CH_2CH_2N), 2.81–2.85 (m, 2H, 2 eq CH_2CH_2N), 3.35 (d, 2 H, J = 2.5 Hz, CCH_2N), and 7.30–7.45 ppm (m, 4 H, C_6H_4Cl); ^{13}C NMR (75 MHz, $CDCl_3$) δ 38.22, 46.97, 48.18, 70.40, 73.27, 78.84, 126.03, 128.34, 132.71, and 146.80 ppm; MS *m/z* (CI) 250 (MH^+, 36), 231 ($M - H_2O$, 95), 139 (60), 94 (100), and 67 (55); HRMS calcd for $C_{14}H_{16}NOCl$ 249.0920, found 249.0919. Anal. Calcd for $C_{14}H_{14}NOCl$: C, 67.33; H, 6.46; N, 5.61. Found: C, 67.13; H, 6.49; N, 5.56.

***N*-Methoxy-*N*-methylbenzamide (13).** Pyridine (2 mL, 5 equiv) and *N*,*O*-dimethylhydroxylamine hydrochloride (490 mg, 5 mmol) were added to a solution of benzoyl chloride (580 μL, 5 mmol) in dry dichloromethane (10 mL). The solution was stirred overnight at room temperature, diluted with dichloromethane (20 mL), washed sequentially with 1 N HCl (20 mL),

saturated sodium bicarbonate (20 mL), and brine (20 mL), and then dried and concentrated under reduced pressure to give **13** as a colorless oil (762 mg, 92.4%). The oil was used without further purification in the next step: IR ($CHCl_3$) 3064, 3029, 3009, 2973, 2958, 1638, and 1574 cm^{-1}; ^1H NMR (300 MHz, $CDCl_3$) δ 3.34, 3.54 (2 s, 2 × 3 H, NCH_3 and OCH_3), and 7.36–7.67 ppm (m, 5 H, C_6H_5); ^{13}C NMR (75 MHz, $CDCl_3$) δ 33.60, 60.84, 127.83, 127.92, 130.37, 133.95, and 169.74 ppm; MS *m/z* (EI) 165 ($M^{\cdot+}$, 1.5), 105 (C_7H_5O, 100), and 77 (C_6H_5, 53); HRMS calcd for $C_9H_{11}NO_2$ 165.0790, found 165.0788.

4-(4′-(4″-Chlorophenyl)-4′-hydroxypiperidinyl)-1-phenylbut-2-yn-1-one (4). Lithium hexamethyldisilazide (2 mL, 1.0 M in tetrahydrofuran, 2 mmol) was added dropwise at 0 °C under argon to a solution of *N*-propargylpiperidine (**12**) (250 mg, 1 mmol) in dry tetrahydrofuran (5 mL). After the reaction mixture was stirred at 0 °C for 10 min, a solution of amide **13** (174 mg, 1.05 mmol) in tetrahydrofuran (3 mL) was added. Stirring was continued for 2 h as the solution was allowed to warm to room temperature. The reaction was then quenched with saturated ammonium chloride solution (10 mL) and diluted with ethyl acetate (30 mL). The organic layer was separated, washed with brine (20 mL), dried, and concentrated under vacuum to give **4** as a solid (363 mg, 102%). The material was pure enough to use in the next step but could be further purified by flash column chromatography (SiO_2, 70% ethyl acetate/hexane) and could be recrystallized from dichloromethane/ether/hexane for analysis: mp 138–139 °C dec; λ_{max} (MeOH) 262, 218 nm; IR ($CHCl_3$) 3444, 3009, 2945, 2833, 2221, 1644, and 1265 cm^{-1}; ^1H NMR (300 MHz, $CDCl_3$) δ 1.79–1.84 (m, 2 H, 2 eq CH_2CH_2N), 2.18 (dt, 2 H, J = 8.5, 13.5 Hz, 2 ax CH_2CH_2N), 2.86–2.89 (m, 4 H, 2 CH_2CH_2N), 3.69 (s, 3 H, CCH_2N) 7.33, 7.46 (AB q, 4 H, J = 8.6 Hz, C_6H_4Cl), 7.50 (t, 2 H, J = 7.5 Hz, 2 *CH*CHCCCO), 7.63 (t, 1 H, J = 7.4 Hz, *para* H of C_6H_5), and 8.18 ppm (d, 1 H, J = 7.6 Hz, 2 CHC*H*CCCO); ^{13}C NMR (75 MHz, $CDCl_3$) δ 38.25, 47.44, 48.43, 70.31, 83.68, 90.38, 126.05, 128.40, 128.57, 129.58, 132.79, 134.14, 136.49, 146.70, and 177.71 ppm; MS *m/z* (CI) 354 (MH^+, 60), 336 ($MH^+ - H_2O$, 100), 194 (29), and 115 (31); HRMS calcd for $C_{21}H_{20}NO_2Cl$ 353.1183, found 353.1173. Anal. Calcd for $C_{21}H_{20}NO_2Cl$: C, 71.28; H, 5.70; N, 3.96. Found: C, 71.19; H, 5.74; N, 3.91.

***N*-(4′,5′-Epoxy-4′-phenylpent-2′-ynyl)-4-(4′-chlorophenyl)-4-piperidinol (3).** Trimethylsulfonium iodide (171 mg, 0.84 mmol) was suspended in dry tetrahydrofuran (5 mL), and *n*-butyllithium (330 μL of a 2.5 M solution in hexanes, 0.82 mmol) was added dropwise at 0 °C under argon. After the mixture was stirred for 10 min, a solution of ynone **4** (100 mg, 0.28 mmol) was added in tetrahydrofuran (3 mL), and the reaction mixture was stirred at 0 °C for 30 min and at room temperature for 30 min. The reaction was quenched by the addition of saturated sodium bicarbonate solution (10 mL) and was then diluted with ethyl acetate (30 mL). The organic layer was separated, washed with brine (20 mL), dried, and concentrated under reduced pressure. The residue was purified by flash column chromatography (SiO_2, 70% ethyl acetate/hexane) to give **3** as a pale yellow oil (39 mg, 38%): IR ($CHCl_3$) 3016, 2924, 2833, 2770, and 1497 cm^{-1}; ^1H NMR (300 MHz, $CDCl_3$) δ 1.75 (d, 2 H, J = 8.6 Hz, 2 eq CH_2CH_2N), 2.13 (td, 2 H, J = 4.5, 13 Hz, 2 ax CH_2CH_2N), 2.68–2.83 (m, 4 H, 2 CH_2CH_2N), 3.01, 3.41 (AB q, 2 H, J = 6.4 Hz, CH_2O), 3.45 (s, 2 H, CCH_2N), and 7.29–7.52 ppm (m, 9 H, C_6H_5 and C_6H_4Cl); ^{13}C NMR (75 MHz, $CDCl_3$) δ 38.45, 47.41, 48.48, 51.10, 58.93, 70.58, 80.05, 83.07, 125.64, 126.12, 128.41, 132.92, 137.43, and 146.91 ppm; MS *m/z* (EI) 367 ($M^{\cdot+}$, 4.5), 349 ($M^{\cdot+} - H_2O$, 4), 189 (73), 158 (31), 139 (31), 129 (100), and 115 (38); HRMS calcd for $C_{22}H_{22}NO_2Cl$ 367.1339, found 367.1322.

The epoxide could also be synthesized by addition of the acetylide anion of **12** to bromoacetophenone. Thus, *N*-propargyl-4-(4′-chlorophenyl)-4-piperidinol (95 mg, 0.38 mmol) was dissolved in dry tetrahydrofuran (4 mL) and cooled to 0 °C under argon. Lithium hexamethyldisilazide (0.84 mL of a 1 M tetrahydrofuran solution, 2.2 equiv) was then added dropwise, and the solution was stirred at 0 °C for 15 min before it was transferred via cannula to a suspension of cerium trichloride (200 mg, 0.8 mmol) in tetrahydrofuran (4 mL) at −78 °C under argon. The cerium suspension had previously been stirred at room temperature for 1 h. After the mixture was stirred for 1 h at −78 °C, phenacyl bromide (112 mg, 1.5 equiv) was added and the reaction was allowed to warm to room temperature. After 4 h, the reaction was quenched with saturated ammonium chloride solution and the aqueous phase was extracted with ethyl acetate (3 × 20 mL). The combined organic extracts were dried and evaporated to yield an oil. The oil was dissolved in methanol, potassium carbonate (140 mg, 1 mmol) was added, and the mixture was stirred at room temperature for 4 h. The solvent was then removed under reduced pressure and the residue partitioned between ethyl acetate (20 mL) and brine (20 mL). The organic layer was separated, dried, and concentrated to give an oil that was purified by flash column chromatography (SiO_2, 60% ethyl acetate/hexane) to give **3** contaminated with an equimolar amount of starting alkyne **12**.

***N*-Methoxy-*N*-methyl-*m*-biphenylcarboxamide (14).** Oxalyl chloride (88 μL, 1.01 mmol) was added with a catalytic amount of DMF (25 μL) to a solution of *m*-biphenylcarboxylic acid (200 mg, 1.01 mmol) in dry dichloromethane (10 mL) under argon. After the mixture was stirred for 15 min, pyridine (1 mL, 5 equiv) and *N,O*-dimethylhydroxylamine hydrochloride (100 mg, 1.01 mmol) were added. The solution was stirred overnight at room temperature and then diluted with dichloromethane (20 mL) and washed sequentially with 1 N HCl (20 mL), saturated sodium bicarbonate (20 mL), and brine (20 mL). It was then dried and concentrated under reduced pressure to give **14** as a colorless oil (182 mg, 74.8%) that was used in the next step without further purification: IR ($CHCl_3$) 3009, 2938, 1638, 1455, 1427, and 1384 cm^{-1}; ^1H NMR (300 MHz, $CDCl_3$) δ 3.37, 3.57 (2 s, 2 × 3 H, NCH_3 and OCH_3), 7.34–7.68 (m, 8 H, C_6H_5 and 3 H of C_6H_4), and 7.91 ppm (s, 1 H, aromatic CCHC); ^{13}C NMR (75 MHz, $CDCl_3$) δ 33.64, 60.94, 126.65, 126.70, 126.95, 127.44, 128.33, 128.69, 129.05, 134.44, 140.15, 140.82, and 169.72 ppm; *m/z* 241 ($M^{\cdot+}$, 3), 211 (3), 198 (5), 181 ($C_{12}H_9CO$, 100), 153 (50), 127 (4), and 76 (8); HRMS calcd for $C_{15}H_{15}NO_2$ 241.1103, found 241.1106.

4-(4′-(4″-Chlorophenyl)-4′-hydroxypiperidinyl)-1-*m*-biphenylbut-2-yn-1-one (5). Lithium hexamethyldisilazide (1.52 mL, 1.0 M in tetrahydrofuran, 1.52 mmol) was added dropwise under argon at 0 °C to a solution of *N*-propargylpiperidine **12** (188 mg, 0.76 mmol) in dry tetrahydrofuran (5 mL). After the reaction mixture was stirred for 10 min at 0 °C, a solution of amide **14** (182 mg, 0.76 mmol) in tetrahydrofuran (5 mL) was added. Stirring was continued for 2 h as the solution was allowed to warm to room temperature. The reaction was quenched with saturated ammonium chloride solution (10 mL) and was then diluted with ethyl acetate (30 mL). The organic layer was separated, washed with brine (20 mL), dried, and concentrated. The residue was purified by flash column chromatography (SiO_2, 40% ethyl acetate/hexane) to give **5** as a solid (146 mg, 45%) that could be recrystallized from dichloromethane/ether/hexane for analysis: mp 130.5–131.5 °C dec; λ_{max} (CH_3OH) 250, 222, and 206 nm; IR ($CHCl_3$) 3016, 2945, 2832, 2214, 1644, and 1595 cm^{-1}; ^1H NMR (300 MHz, $CDCl_3$) δ 1.76 (brd d, 2 H, J = 12.6 Hz, 2 eq CH_2CH_2N), 1.88 (brd s, 1 H, OH), 2.09–2.19 (m, 2 H, 2 ax CH_2CH_2N), 2.85–2.89 (m, 4 H, 2 CH_2CH_2N), 3.67 (s, 2 H, NCH_2C), 7.29–7.84 (m, 10 H, ClC_6H_4, C_6H_5 and $CHCHCC_6H_5$), 7.83 (d, 1 H, J = 7.7 Hz, $CHCHCC_6H_5$), 8.14 (d, 1 H, J = 7.7 Hz, $CHCHCCO$), and 8.41 ppm (s, 1 H, CCHCCO); ^{13}C NMR (75 MHz, $CDCl_3$) δ 38.23, 47.44, 48.36, 70.24, 83.81, 90.62, 125.97, 127.18, 127.86, 128.28, 128.37, 128.88, 129.05, 132.74, 136.98, 139.86, 141.64, 146.70, and 177.59 ppm; MS *m/z* 429 ($M^{\cdot+}$, 47), 411 ($M^{\cdot+} - H_2O$, 14), 231 (83), 181 ($C_{12}H_9CO$, 100), 153 ($C_{12}H_9$, 57), 152 (59), and 94 (60); HRMS calcd for $C_{27}H_{44}NO_2Cl$ 429.1496, found 429.1500. Anal. Calcd for $C_{27}H_{24}NO_2Cl$: C, 75.43; H, 5.63; N, 3.26. Found: C, 75.34; H, 5.73; N, 3.18.

***N*-Methoxy-*N*-methyl-*p*-biphenylcarboxamide (15).** Pyridine (4 mL, 5 equiv) and *N,O*-dimethylhydroxylamine hydrochloride (980 mg, 10 mmol) were added to a solution of *p*-biphenylcarbonyl chloride (2.16 g, 10 mmol) in dry dichloromethane (10 mL). The solution was stirred for 2 h at room temperature, diluted with ethyl acetate (20 mL), and washed sequentially with 1 N HCl (2 × 20 mL), saturated sodium bicarbonate (20 mL), and brine (20 mL). It was then dried over magnesium sulfate and evaporated under reduced pressure to give **15** as a solid (1.78 g, 74%) that could be recrystallized from ethyl acetate/hexane for analysis: mp 77–78 °C; IR ($CHCl_3$) 3030, 2973, 2938, 1630, 1420, and 1384 cm^{-1}; ^1H NMR (300 MHz, $CDCl_3$) δ 3.38, 3.59 (2 s, 2 × 3 H, NCH_3 and OCH_3) and 7.34–7.79 ppm (m, 9 H, C_6H_5 and C_6H_4); ^{13}C NMR (75 MHz, $CDCl_3$) δ 33.76, 61.05, 126.62, 127.11, 127.78, 128.80, 132.67, 140.15, 143.32, and 169.62 ppm; MS *m/z* (EI) 241 ($M^{\cdot+}$, 3), 211 (4), 198 (7), 181

($C_6H_5C_6H_4CO$, 100), 152 (44), and 76 (7); HRMS calcd for $C_{15}H_{15}NO_2$ 241.1103, found 241.1116. Anal. Calcd for $C_{15}H_{15}NO_2$: C, 74.67; H, 6.27; N, 5.80. Found: C, 74.70; H, 6.25; N, 5.55.

4-(4′-(4″-Chlorophenyl)-4′-hydroxypiperidinyl)-1-*p*-biphenylbut-2-yn-1-one (6). *N*-Propargylpiperidine **12** (252 mg, 1 mmol) was dissolved in dry tetrahydrofuran (10 mL) at room temperature under argon, and lithium hexamethyldisilazide (2.5 mL, 1.0 M in tetrahydrofuran, 2.5 mmol) was added dropwise. After the reaction mixture was stirred for 20 min, amide **15** (410 mg, 1.7 mmol) was added. The solution was then heated at reflux for 1 h. After the reaction mixture was cooled to room temperature, the reaction was quenched with saturated ammonium chloride solution (10 mL) and diluted with ethyl acetate (30 mL). The organic layer was separated, washed with brine (20 mL), dried, and evaporated to dryness. The residue was purified by flash column chromatography (SiO_2, 2% 2-propanol/dichloromethane). The product-containing fractions were rechromatographed (SiO_2, 40% ethyl acetate/hexane) to give **6** as a solid (285 mg, 66%) that could be recrystallized from dichloromethane/hexane for analysis: mp 168–169 °C dec; λ_{max} (CH_3OH) 308, 222, and 206 nm; IR ($CHCl_3$) 3023, 2945, 2833, 2221, 1644, 1602, and 1265 cm^{-1}; ^1H NMR (300 MHz, $CDCl_3$) δ 1.82 (brd d, 2 H, J = 14 Hz, 2 eq CH_2CH_2N), 2.12–2.22 (m, 2 H, 2 ax CH_2CH_2N), 2.86–2.90 (m, 4 H, 2 CH_2CH_2N), 3.69 (s, 2 H, NCH_2C), 7.30–7.72 (m, 11 H, ClC_6H_4, C_6H_5 and 2 $CHCC_6H_5$), and 8.24 ppm (d, 2 H, J = 8.8 Hz, 2 $CHCHCC_6H_5$); ^{13}C NMR (75 MHz, $CDCl_3$) δ 38.24, 47.47, 48.43, 70.28, 83.89, 90.34, 126.08, 127.28, 128.43, 128.96, 130.22, 132.80, 135.34, 139.60, 146.72, 146.88, and 177.34 ppm. Anal. Calcd for $C_{27}H_{24}NO_2Cl$: C, 75.43; H, 5.63; N, 3.26. Found: C, 75.55; H, 5.70; N, 3.12.

4-(4′-(4″-Chlorophenyl)-4′-hydroxypiperidinyl)-1-phenyl-2-(phenylselenyl)butan-1-one (16). Lithium hexamethyldisilazide (1 M, 0.665 mmol) was added at −78 °C to a solution of haloperidol (100 mg, 0.266 mmol) in tetrahydrofuran (5 mL), and the mixture was stirred at room temperature for 2 h before it was cooled to −78 °C and a solution of benzeneselenyl chloride (57.5 mg, 0.3 mmol) in tetrahydrofuran (3 mL) was added. The reaction mixture was stirred at room temperature for 2 h, poured into water, and extracted with ethyl acetate. The extract was dried over magnesium sulfate. Compound **16** was obtained as a colorless oil (101 mg, 73.5%) by column chromatography (silica gel, ethyl acetate): ^1H NMR (300 MHz, $CDCl_3$) δ 1.55 (d, CH_2CH_2N eq), 1.68–1.77 (m, 2H, $CH_2CH_2CH_2$) 1.79 (s, br, OH), 2.05 (m, 2H, CH_2CH_2N ax), 2.24 (t, 2H, CH_2CH_2N ax), 2.46 (m, 2H, CH_2N chain), 2.63 (d, 2H, CH_2CH_2N eq), 4.61 (m, 1H, CHSe), 7.07 (t, J = 7 Hz, 2H, FCCH), 7.21–7.48 (m, 9H, SePh, ClPh), and 7.90 ppm (dd, J = 5, 8 Hz, 2H, FCCHCH); ^{13}C NMR (75 MHz, $CDCl_3$) δ 29.5 (CH_2CH_2CH), 38.0 (CH_2CH_2N of piper.), 44.1, 49.9 (CH_2N), 56.6 (CHSe), 70.8 (COH), 115.5 (d, J = 21 Hz, FCCH), 128.5 (d, J = 6 Hz, FCCHCH), 129.0, 130.8, 130.9, 132.6, 133.0, 136.1, 146.9 (CHPh, SePh, FCCHCHC), 165.4 (d, J = 254 Hz, FC), and 193.9 ppm (C=O); MS (CI) m/z 376 (M − FPhCO − OH, 15), 314 (34), 237 (100), 224 (95), 157 (63), 123 (FPhCO, 91), and 95 (FPh, 32).

4-(4′-(4″-Chlorophenyl)-4′-hydroxy-1-oxopiperidinyl)-1-phenylbut-2-en-1-one (7). H_2O_2 (30%) (0.15 mL, ca. 1.3 mmol) was added to a solution of (phenylselenyl)haloperidol **16** (85 mg, 0.164 mmol) in tetrahydrofuran (1.5 mL) and acetic acid (60 μL) at 0 °C. The mixture was stirred at 0 °C for 2 h and then at 25 °C for 2 h before saturated sodium bicarbonate was added. The precipitate that formed was collected by filtration and dried under vacuum. Compound **7** was thus obtained as a white solid (42 mg, 65.7%): mp 135 °C dec; IR (KBr) 3082, 1680, 1629, and 1598; ^1H NMR (300 MHz, $CDCl_3$) δ 1.72 (d, CH_2CH_2N eq), 2.75 (m, 2H, CH_2CH_2N ax), 3.22 (d, 2H, CH_2CH_2N ax), 3.30 (m, 3H, CH_2N, CH=), 3.79 (d, 2H, CH_2CH_2N eq), 4.25 (d, J = 8 Hz, 1H, H-3), 7.24–7.56 (m, 6H, FCCH, ClPh), and 8.12 ppm (m, 2H, FCCHCH); MS (CI) m/z 371 ($M^+ - H_2O$, 9), 189 (100), 178 (91), 154 (66), 123 (FPhCO, 98), and 95 (FPh, 99); MS (LSIMS) 390 (M + H^+, 19). Anal. Calcd for $C_{21}H_{21}NO_3ClF$: C, 64.70; H, 5.43; N, 3.59. Found: C, 64.31; H, 5.54; N, 3.34.

4-(4′-(4″-Chlorophenyl)-4′-hydroxypiperidinyl)-1-phenylbut-2-en-1-one (8). *m*-Chloroperbenzoic acid (19 mg, 80–90%, ≈0.1 mmol) was added at 0 °C to a solution of α-(phenylselenyl)-haloperidol **16** (52 mg, 0.1 mmol) in dichloromethane (4 mL). The solution was stirred at this temperature for 6 h before aqueous sodium bicarbonate and 10 mL of CH_2Cl_2 were added and the organic phase was separated and dried over $MgSO_4$. After solvent removal, the residue was purified by column chromatography (silica gel, ethyl acetate/hexane = 7/3). Compound **8** was obtained as a colorless oil (16 mg, 42.8%): IR (NaCl) 3058, 2951, 1688, 1598, and 1270; ^1H NMR (300 MHz, $CDCl_3$) δ 1.73 (s, 1 H, OH), 1.75 (d, 2 H, CH_2CH_2N, eq), 2.15 (t, 2 H, CH_2CH_2N, ax), 2.55 (t, 2 H, CH_2CH_2N, ax), 2.84 (d, 2 H, CH_2CH_2N, eq), 3.33 (d, 2H, NCH_2), 7.07 (m, 2H, =CH), 7.15 (t, 2 H, CHCHCF), 7.33/7.45 (2 d, 4 H, ClC_6H_5), and 7.99 ppm (m, 2 H, CHCF); ^{13}C NMR (75 MHz, $CDCl_3$) δ 38.37, 49.59, 59.85, 70.76, 115.68, 125.99, 127.01, 128.39, 130.57, 131.12, 132.82, 133.89, 145.64, 146.63, 165.52, and 188.78 ppm; MS m/z (EI) 373 (16), 371 (22), 250 (25), 189 (27), and 123 (100); HRMS calcd for $C_{21}H_{21}ClFNO_2$ 373.1245, found 373.1165.

4-(4′-(4″-Chlorophenyl)-4′-hydroxypiperidinyl)-3-((2′-hydroxyethyl)thio)-1-phenyl-2-buten-1-one (9). Acetylenic ketone **4** (50 mg, 0.14 mmol) was dissolved in methanol (1 mL) with β-mercaptoethanol (10 μL, 0.14 mmol), and the reaction mixture was stirred overnight at room temperature. The mixture was then concentrated to dryness and the residue purified by flash column chromatography (SiO_2, 60% ethyl acetate/hexane) to give **9** (39 mg, 63.9%) as a pale yellow solid which could be recrystallized from dichloromethane/ether/hexane for analysis: mp 122.5–123.5 °C; λ_{max} (MeOH) 338, 258, 220, and 206 nm; IR ($CHCl_3$) 3023, 2931, 2840, 1630, and 1532 cm^{-1}; ^1H NMR (300 MHz, $CDCl_3$) δ 1.75 (brd d, 2 H, J = 13 Hz, 2 eq CH_2CH_2N), 2.13 (dt, 2 H, J = 4, 13 Hz, 2 ax CH_2CH_2N), 2.59 (brd t, 2 H, J = 11 Hz, 2 ax CH_2CH_2N), 2.89 (brd d, 2 H, J = 11 Hz, 2 eq CH_2CH_2N), 3.17 (t, 2 H, J = 5.4 Hz, CH_2CH_2S), 3.47 (s, 2 H, NCH_2C), 3.84 (t, 2 H, J = 5.4 Hz, CH_2CH_2S), 7.10 (s, 1 H, CH=CS), 7.27–7.52, and 7.91–7.93 ppm (2 m, 7, 2 H, 2 C_6H_4); ^{13}C NMR (75 MHz, $CDCl_3$) δ 33.68, 37.59, 48.50, 61.60, 63.42, 70.57, 120.05, 126.10, 127.92, 128.35, 128.51, 132.33, 132.82, 138.32, 146.31, 158.05, and 188.38 ppm; MS m/z (EI) 429 ($M^{\bullet+}$ − 2, 25), 413 ($M^{\bullet+} - H_2O$, 12), 353 (100), 224 (91), 189 (55), and 105 (C_6H_5CO, 75). Anal. Calcd for $C_{23}H_{26}NO_2ClS$: C, 63.95; H, 6.07; N, 3.24. Found: C, 64.16; H, 6.19; N, 3.18.

Kinetics of the Reactions of Inhibitors with Glutathione and Sodium Acetate. Solutions of glutathione were prepared by weighing into a volumetric flask. Buffers were standardized at 37 °C, and ionic strength was maintained at 1 mM by adding sodium chloride when necessary. The reactions of **4** and **9** with glutathione were monitored by the increase and decrease, respectively, in absorbance at 340 nm and, that of **7** by the change in absorbance at 268 nm. Each data point was determined in triplicate at 37 ± 0.1 °C. Typical reactions were 0.2 mM in electrophile and 7–30 mM in glutathione and were initiated by adding a solution of the nucleophile. No change in the chromophore was observed in incubations without added nucleophiles, indicating that water addition did not occur at a significant rate. The data was analyzed to give a pseudo-first-order rate constant that was converted, using the known glutathione concentration, into the second-order rate constant k_2 for the reaction. In some experiments, glutathione was replaced in the incubations by sodium acetate (50 mM), and the rate of the reaction was monitored by measuring the change in absorbance at 270 nm.

***In Vitro* Assay of HIV Protease Inhibition.** Recombinant HIV-1 PR was expressed in *E. coli* strain D1210 using the pSOD/PR179 vector.[33] Recombinant HIV-2 PR was expressed in *E. coli* strain X90 using the pT2HIV2/115 vector.[34] The enzymes were purified to homogeneity, as judged by a single band on a silver-stained sodium dodecyl sulfate polyacrylamide gel, using a combination of ion-exchange chromatography and affinity chromatography on pepstatin-A agarose. Concentrations of active HIV-1 and HIV-2 enzymes were determined by active-site titration using the peptidomimetic inhibitor U-85548 (a gift of Dr. A. Tomasselli, Upjohn), Val-Ser-Gln-Asn-Leu-Y[CH(OH)-CH_2]-Val-Ile-Val.[35]

Both HIV-1 PR and HIV-2 PR were assayed against the decapeptide Ala-Thr-Leu-Asn-Phe-Pro-Ile-Ser-Pro-Trp, which corresponds to the HIV-1 PR C-terminal autoprocessing site. The decapeptide was synthesized by conventional solid-state methods. Reactions were carried out as described.[14] Conversion of the decapeptide to the two pentapeptides was quantitated by integration of the peak areas after separation on HPLC and comparison with product standard curves. The IC_{50} determinations were carried out at pH 5.5. Stock solutions (1 μM–50

mM) of the inhibitors were prepared in neat DMSO. Compounds were added to assay solutions containing additional DMSO to give a final concentration of 5% (v/v). Baseline values were determined from enzymatic reactions containing 5% DMSO with no inhibitor present. HIV-1 PR and HIV-2 PR were preincubated with the different inhibitors for 5 min at 25 °C, followed by addition of the decapeptide substrate (250 μM final concentration) to initiate the reaction.

For the quantification of irreversible inactivation, HIV-1 PR (1.5 μg/mL final concentration) or HIV-2 PR (80 μg/mL final concentration) was preincubated in the presence of 200 μM of each inhibitor at 37 °C in 50 mM Hepes buffer (pH 8.0) containing 1 M NaCl, 1 mM EDTA, and 5% DMSO. For HIV-1 PR, 100 μM DTT was also added. At various times, aliquots were removed and assayed for activity. Baseline values were determined from enzymatic reactions carried out in the absence of inhibitors.

HIV-1 PR was assayed against the fluorescent substrate ABZ-Thre-Ile-NLe-Phe(*p*-NO_2)-Gln-Arg-NH_2. The enzyme was assayed at pH 6.5 in the absence of NaCl as described previously.[36] HIV-2 PR was assayed against the spectrophotometric substrate NH_2-Arg-Val-Nle-Phe(*p*-NO_2)-Glu-Ala-Nle-Ser-$CONH_2$. The enzyme was assayed in 50 mM sodium acetate buffer (pH 5.5) containing 1 M NaCl and 1 mM EDTA, as described previously.[37] Kinetic data were fitted to a pseudo-first-order equation to calculate the rates of inactivation.

***Ex Vivo* Assay of HIV-1 Protease Inhibition.** An HIV vector system designed to produce replication-defective virions was used to measure the effect of inhibitors on capsid polyprotein processing as well as on viral infectivity *ex vivo*. Virions were produced by cotransfection of COS-7 cells with two expression vectors.[38] One SV40-based vector consists of the HIV proviral genome in which the gp160 sequences were replaced by the guanidyl phosphate ribosyltransferase (*gpt*) gene. The other vector contains the gp160 sequences. Since the virions produced are capable of infecting CD4 positive cells, the number of infectious particles can be quantitated by placing infected cells under selective pressure and counting drug-resistant colonies. A compound able to inhibit the HIV-1 protease would specifically exert its effect during virus assembly and processing. To measure this effect, the transfected cells were treated with various inhibitors for short periods of time and the culture supernatant was collected to measure infectious particles as well as levels of capsid protein processing. The concentrations chosen for the *ex vivo* inhibition trials were based on the IC_{50} values obtained *in vitro* and the effects of the compounds on cell viability. The length of time the cells could be exposed to the compounds was limited by their cellular toxicity. Under the conditions used in these experiments, a 0.75 μM concentration of peptidomimetic inhibitor U75875 reduced viral titer by 50%.[39]

The cytotoxic effect of the inhibitors was determined using the MTT stain viability assay.[40] The LD_{50} values, defined as the concentrations that reduce viability by 50%, were determined for all the compounds after 4- or 24-h incubation periods (Table 3). Due to the toxicity of most of the compounds, the incubation periods for viral assays were restricted to 4 h. Following incubation of virus-producing cells with various concentrations of the test compounds, the virus particles were isolated by ultracentrifugation. These particles were disrupted using Triton X-100, and the amount of p24 capsid protein was quantitated by ELISA. The effects on p24 levels reported in Table 3 were obtained at drug concentrations that had no detectable effect on cell viability.

Cells Lines and Vectors. COS-7 and HeLa/T4 cells were maintained in DME H21 media supplemented with 10% dialyzed fetal calf serum (Gibco, Long Island, NY) and antibiotics (100 units/mL penicillin G, 100 μg/mL streptomycin sulfate). Plasmids HIV-gpt and HXB2-env were kindly provided by K. Page and D. Littman (University of California, San Francisco).[38]

MTT Cell Viability Assay. This is a quantitative colorimetric assay for mammalian cell survival and proliferation.[40] Cells were seeded in 96-well plates and grown to near 50% confluency. A serial dilution (1–500 μM) of each compound was then prepared in culture media and added (250 μL/well) in duplicate. All culture media was adjusted to a final concentration of 1.0% DMSO (v/v). The cells were allowed to grow for either 4 or 24 h. The culture media was then removed, and the cells were washed with phosphate-buffered saline (PBS) before 50 μL of MTT solution (1 mg/mL in PBS) was added. After incubating for 4 h at 37 °C, the reaction was quenched by adding 160 μL of acidified 2-propanol and mixing to dissolve purple crystals. The absorbance was determined within 30 min at 570 nm on an ELISA plate reader. LD_{50} values for each compound were then determined from a plot of the average of the observed absorbance versus the concentration of the inhibitor.

Production of Virus. Virus was generated by cotransfection of plasmid DNA HIV-gpt and HXB2-env into COS-7 cells by the calcium phosphate procedure with the following modifications.[41] Twenty micrograms of each plasmid was added to 10-cm dishes of cells at 50% confluency in the presence of 100 μM chloroquine. Following overnight incubation, the culture media was replaced. Virus production was detectable within 12 h and peaked between 48 and 65 h posttransfection.

Drug Treatment. The compounds were added 48 h post-transfection, at the peak of virus production, and the incubation was restricted to a 4-h period. Due to their low solubility in aqueous solutions, concentrated stock solutions (generally 50 mM) were prepared in neat DMSO. Culture media was adjusted to the desired concentration of these compounds just prior to its addition to cells. To avoid precipitation, the compounds were aliquoted first to a tube in sufficient DMSO to yield a 1.0% final concentration, and subsequently the culture media was added quickly and vortexed. The culture media was collected after a 4-h incubation of the cells with each of the compounds. This culture supernatant is the source of virus for measurement of infectivity as well as levels of p24 and other capsid proteins.

Infectivity Measurements. HeLa/T4 cells were seeded at 2.5×10^5 cells/culture well. A 500-μL aliquot of culture media containing the virus to be titered was then added (using dilutions of 1:2, 1:5, and 1:20). The virus was then allowed to be absorbed for 45 min at 37 °C. The supernatant was aspirated, and 1.5 mL of fresh media was added to the culture overnight. Selective media containing 50 μg/mL mycophenolic acid (CalBiochem), 14 μg/mL hypoxanthine, and 250 μg/mL xanthine was then added, and the selection was allowed to take place for 12–14 days during which cells expressing the gpt gene survived and formed colonies. The colonies were then stained with 0.5% crystal violet and 1% formaldehyde in a 1:1 ethanol/PBS solution. The colonies were counted, and the average was determined from duplicate wells. The reduction in infectivity was calculated as a percentage of colonies from treated versus untreated cells in duplicate wells.

p24 Core Antigen ELISA Assay. An ELISA kit purchased from NEN/DuPont was used to determine the amount of p24 present in culture media or virus preparations. This capture assay uses a monoclonal antibody that preferentially binds p24 while it reacts with larger capsid protein precursors to a very limited extent. The assay was carried out using the manufacturer's indications. Samples were pretreated with 1% Triton to inactivate the virus.

Virus Isolation by Ultracentrifugation. The culture medium was filtered through a 0.45-μm syringe filter and was then centrifuged to remove any precipitate. The medium was then spun through a cushion of 20% sucrose in PBS in an SW41 Beckman rotor for 1.5 h at 35 K and 4 °C. The pelleted material was collected.

Acknowledgment. This work was supported by National Institutes of Health Grant GM 39552. The Computer Graphics and Mass Spectrometry Facilities are supported by the Division of Research Resources of the National Institutes of Health.

References

(1) Darke, P. L.; Leu, C.-T.; Davis, L. J.; Heimbach, J. C.; Diehl, R. E.; Hill, W. S.; Dixon, R. A. F.; Sigal, I. S. Human Immunodeficiency Virus Protease. Bacterial Expression and Characterization of the Purified Aspartic Protease. *J. Biol. Chem.* **1989**, *264*, 2307–2312.
(2) Wlodawer, A.; Miller, M.; Jaskólski, M.; Sathyanarayana, B. K.; Baldwin, E.; Weber, I. T.; Selk, L. M.; Clawson, L.; Schneider, J.; Kent, S. B. H. Conserved Folding in Retroviral Proteases: Crystal Structure of a Synthetic HIV-1 Protease. *Science* **1989**, *245*, 616–621.
(3) Navia, M. A.; Fitzgerald, P. M. D.; McKeever, B. M.; Leu, C.-T.; Haimbach, J. C.; Herber, W. K.; Sigal, I. S.; Darke, P. L.; Springer, J. P. Three-Dimensional Structure of Aspartyl Protease from Human Immunodeficiency Virus HIV-1. *Nature* **1989**, *337*, 615–620.

(4) Lapatto, R.; Blundell, T.; Hemmings, A.; Overington, J.; Wilderspin, A.; Wood, S.; Merson, J. R.; Whittle, P. J.; Danley, D. E.; Geoghegan, K. F.; Hawrylik, S. J.; Lee, S. E.; Scheld, K. G.; Hobart, P. M. X-Ray Analysis of HIV-1 Proteinase at 2.7 Å Resolution Confirms Structural Homology Among Retroviral Enzymes. *Nature* **1989**, *342*, 299–302.
(5) Mulichak, A. M.; Hui, J. O.; Tomasselli, A. G.; Heinrikson, R. L.; Curry, K. A.; Tomich, C. S.; Thaisrivongs, S.; Sawyer, T. K.; Watenpaugh, K. D. The Crystallographic Structure of the Protease from Human Immunodeficiency Virus Type 2 with Two Synthetic Peptidic Transition State Analog Inhibitors. *J. Biol. Chem.* **1993**, *268*, 13103–13109.
(6) Farmerie, W. C.; Loeb, D. D.; Casavant, N. C.; Hutchison, C. A., III; Edgell, M. H.; Swanstrom, R. Expression and Processing of the AIDs Virus Reverse Transcriptase in *Escherichia coli*. *Science* **1987**, *236*, 305–308.
(7) Kohl, N. E.; Emini, E. A.; Schleif, W. A.; Davis, L. J.; Heimbach, J. C.; Dixon, R. A. F.; Scolnick, E. M.; Sigal, I. S. Active Human Immunodeficiency Virus Protease is Required for Viral Infectivity. *Proc. Natl. Acad. Sci. U.S.A.* **1988**, *85*, 4686–4690.
(8) McQuade, T. J.; Tomasselli, A. G.; Liu, L.; Karacostas, V.; Moss, B.; Sawyer, T. K.; Heinrikson, R. L.; Tarpley, W. G. A Synthetic HIV-1 Protease Inhibitor with Antiviral Activity Arrests HIV-like Particle Maturation. *Science* **1990**, *247*, 454–456.
(9) Roberts, N. A.; Martin, J. A.; Kinchington, D.; Broadhurst, A. V.; Craig, J. C.; Duncan, I. B.; Galpin, S. A.; Handa, B. K.; Kay, J.; Kröhn, A.; Lambert, R. W.; Merrett, J. H.; Mills, J. S.; Parkes, K. E. B.; Redshaw, S.; Ritchie, A. J.; Taylor, D. L.; Thomas, G. J.; Machin, P. J. Rational Design of Peptide-based HIV Proteinase Inhibitors. *Science* **1990**, *248*, 358–361.
(10) Rich, D. H.; Green, J.; Toth, M. V.; Marshall, G. R.; Kent, S. B. H. Hydroxyethylamine analogues of the p17/p24 substrate cleavage site are tight-binding inhibitors of HIV protease. *J. Med. Chem.* **1990**, *33*, 1285–1288.
(11) Meek, T. D.; Lambert, D. M.; Dreyer, G. B.; Carr, T. J.; Tomaszek, T. A., Jr.; Moore, M. L.; Strickler, J. E.; Debouck, C.; Hyland, L. J.; Matthews, T. J.; Metcalf, B. W.; Petteway, S. R. Inhibition of HIV-1 Protease in Infected T-Lymphocytes by Synthetic Peptide Analogues. *Nature (London)* **1990**, *343*, 90–92.
(12) Schnebli, H. P.; Braun, N. J. Proteinase Inhibitors as Drugs. In *Proteinase Inhibitors*; Barret, A. J., Salvesen, G. S., Eds.; Elsevier Science Publishers: New York, 1986; pp 613–627.
(13) Cressman, W. A.; Bianchine, J. R.; Slotnick, V. B.; Johnson, P. C.; Plostnieks, J. Plasma Level Profile of Haloperidol in Man Following Intramuscular Administration. *Eur. J. Clin. Pharmacol.* **1974**, *7*, 99–103.
(14) DesJarlais, R. L.; Seibel, G. L.; Kuntz, I. D.; Ortiz de Montellano, P. R.; Furth, P. S.; Alvarez, J. C.; DeCamp, D. L.; Babé, L. M.; Craik, C. S. Structure-based Design of Nonpeptide Inhibitors Specific for the Human Immunodeficiency Virus 1 Protease. *Proc. Natl. Acad. Sci. U.S.A.* **1990**, *87*, 6644–6648.
(15) Rutenber, E.; Fauman, E. B.; Keenan, R. J.; Fong, S.; Furth, P. S.; Ortiz de Montellano, P. R.; Meng, E.; Kuntz, I. D.; DeCamp, D. L.; Salto, R.; Rosé, J. R.; Craik, C. S.; Stroud, R. M. Structure of a Non-Peptide Inhibitor Complexed with HIV-1 Protease. Developing a Cycle of Structure-Based Drug Design. *J. Biol. Chem.* **1993**, *268*, 15343–15346.
(16) Lewi, P. J.; Heykants, J. J. P.; Allewijn, F. T. N.; Dony, J. G. H.; Janssen, P. A. J. Distribution and Metabolism of Neuroleptic Drugs: Part I. Pharmacokinetics of Haloperidol. *Arzneim.-Forsch.* **1970**, *20*, 943–948.
(17) Davies, D. R. The Structure and Function of the Aspartic Proteinases. *Annu. Rev. Biophys. Biophys. Chem.* **1990**, *19*, 189–215.
(18) Rich, D. H. Pepstatin-Derived Inhibitors of Aspartic Proteinases. A Close Look at an Apparent Transition-State Analogue Inhibitor. *J. Med. Chem.* **1985**, *28*, 263–273.
(19) Hyland, L. J.; Tomaszek, T. A.; Roberts, G. D.; Carr, S. A.; Magaard, V. W.; Bryan, H. L.; Fakhoury, S. A.; Moore, M. L.; Minnich, M. D.; Culp, J. S.; DesJarlais, R. L.; Meek, T. D. Human Immunodeficiency Virus-1 Protease. 1. Initial Velocity Studies and Kinetic Characterization of Reaction Intermediates by ^{18}O Isotope Exchange. *Biochemistry* **1991**, *30*, 8441–8453.
(20) Hyland, L. J.; Tomaszek, T. A.; Meek, T. D. Human Immunodeficiency Virus-1 Protease. 2. Use of pH Rate Studies and Solvent Kinetic Isotope Effects to Elucidate Details of Chemical Mechanism. *Biochemistry* **1991**, *30*, 8454–8463.
(21) Meek, T. D.; Dayton, B. D.; Metcalf, B. W.; Dreyer, G. B.; Strickler, J. E.; Gorniak, J. G.; Rosenberg, M.; Moore, M. L.; Magaard, V. W.; Debouck, C. Human Immunodeficiency Virus 1 Protease Expressed in *Escherichia coli* Behaves as a Dimeric Aspartate Protease. *Proc. Natl. Acad. Sci. U.S.A.* **1989**, *86*, 1841–1845.
(22) Chen, K. C. S.; Tang, J. Amino Acid Sequence around the Epoxide-reactive Residues in Pepsin. *J. Biol. Chem.* **1972**, *247*, 2566–2574.
(23) James, M. N. G.; Hsu, I. N.; Delbaere, L. T. J. Mechanism of Acid Proteinase Catalysis Based on the Crystal Structure of Penicillopepsin. *Nature* **1977**, *267*, 808–813.
(24) Blumenstein, J. J.; Copeland, T. D.; Oroszlan, S.; Michejda, C. J. Synthetic Non-Peptide Inhibitors of HIV Protease. *Biochem. Biophys. Res. Commun.* **1989**, *163*, 980–987.
(25) Moelling, K.; Schulze, T.; Knoop, M.-T.; Kay, J.; Jupp, R.; Nicolaou, G.; Pearl, L. H. *In Vitro* Inhibition of HIV-1 Proteinase by Cerulenin. *FEBS Lett.* **1990**, *261*, 373–377.
(26) During the preparation of the manuscript, inactivation of HIV-1 PR by a peptidyl epoxide was also reported: Grant, S. K.; Moore, M. L.; Fakhoury, S. A.; Tomaszek, T. A.; Meek, T. D. Inactivation of HIV-1 Protease by a Tripeptidyl Epoxide. *Bioorg. Med. Chem.* **1992**, *2*, 1441–1445.
(27) Hernandez, O.; Bend, J. R. Metabolism of Epoxides. In *Metabolic Basis of Detoxication*; Jacoby, W. B., Bend, J. R., Caldwell, J., Eds.; Academic Press: New York, 1982, pp 207–228.
(28) Imamoto, T.; Kusumoto, T.; Tawarayama, Y.; Sugiura, Y.; Mita, T.; Hatanaka, Y.; Yokoyama, M. Carbon-Carbon Bond-Forming Reactions Using Cerium Metal or Organocerium(III) Reagents. *J. Org. Chem.* **1984**, *49*, 3904–3912.
(29) Nahm, S.; Weinreb, S. M. N-Methoxy-N-methylamides as Effective Acylating Agents. *Tetrahedron Lett.* **1981**, *22*, 3815–3818.
(30) Corey, E. J.; Chaykovsky, M. Dimethyloxosulfonium Methylide ($(CH_3)_2SOCH_2$) and Dimethylsulfonium Methylide ($(CH_3)_2SCH_2$). Formation and Application to Organic Synthesis. *J. Am. Chem. Soc.* **1965**, *87*, 1353–1364.
(31) Janssen, P. A. J.; Van de Westerringh, C.; Jageneau, A. H. M.; Demoen, P. J. A.; Hermans, B. F. K.; Van Daele, G. H. P.; Schellekens, K. H. L.; Van Der Eycken, C. A. M.; Niemegeers, C. J. E. Chemistry and Pharmacology of CNS Depressants Related to 4-(4-hydroxy-4-phenylpiperidino)butyrophenone. Part I. Synthesis and Screening Data in Mice. *J. Med. Pharm. Chem.* **1959**, *1*, 281–297.
(32) Salto, R.; Babé, L. M.; Li, J.; Rosé, J. R.; Yu, Z.; De Voss, J. J.; Sui, Z.; Ortiz de Montellano, P. R.; Craik, C. S. *In Vitro* Characterization of Non-Peptide Irreversible Inhibitors of HIV Proteases. *J. Biol. Chem.* In press.
(33) Babé, L. M.; Pichuantes, S.; Barr, P. J.; Bathurst, I.; Masiarz, F. R.; Craik, C. S. HIV 1 Protease: Bacterial Expression, Purification, and Characterization. In *Proteins and Pharmaceutical Engineering*; Craik, C. S., Fletterick, R., Matthews, C. R., Wells, J., Eds.; Wiley-Liss: New York, 1990; Vol. 110; pp 71–88.
(34) Rosé, J.; Salto, R.; Craik, C. S. Regulation of Autoproteolysis of the HIV-1 and HIV-2 Proteases with Engineered Amino Acid Substitutions. *J. Biol. Chem.* **1993**, *268*, 11939–11945.
(35) Tomasselli, A. G.; Olsen, M. K.; Hui, J. O.; Staples, D. J.; Sawyer, T. K.; Heinrikson, R. L.; Tomich, C.-S. Substrate Analogue Inhibition and Active Site Titration of Purified Recombinant HIV-1 Protease. *Biochemistry* **1990**, *29*, 264–269.
(36) Toth, M. V.; Marshall, G. R. A Simple, Continuous Fluorometric Assay for HIV Protease. *Int. J. Peptide Protein Res.* **1990**, *36*, 544–550.
(37) Richards, A. D.; Phylip, L. H.; Farmerie, W. G.; Scarborough, P. E.; Alvarez, A.; Dunn, B. M.; Hirel, P.-H.; Konvalinka, J.; Strop, P.; Pavlickova, L.; Kostka, V.; Kay, J. Sensitive, Soluble Chromogenic Substrates for HIV-1 Proteinase. *J. Biol. Chem.* **1990**, *265*, 7733–7736.
(38) Page, K. A.; Landau, N. R.; Littman, D. R. Construction and Use of a Human Immunodeficiency Virus Vector for Analysis of Virus Infectivity. *J. Virol.* **1990**, *265*, 5270–5276.
(39) Ashorn, P.; McQuade, T. J.; Thaisrivongs, S.; Tomasselli, A. G.; Tarpley, W. G.; Moss, B. An Inhibitor of the Protease Blocks Maturation of Human and Simian Immunodeficiency Viruses and Spread of Infection. *Proc. Natl. Acad. Sci. U.S.A.* **1990**, *87*, 7472–7476.
(40) Mossman, T. Rapid Colorimetric Assay for Cellular Growth and Survival: Application to Proliferation and Cytotoxicity Assays. *J. Immunol. Meth.* **1983**, *65*, 55–63.
(41) Graham, F. L.; van der Eb, J. A. New Technique for the Assay of Human Adenovirus 5 DNA. *Virology* **1973**, *52*, 456–467.